

Aim and Scope

The *Journal of Applied Packaging Research* is an international forum for the dissemination of research papers, review articles, tutorials and news about innovative or emerging technologies for the packaging industry. The journal is targeted towards the broad packaging community including packaging scientists and engineers in industry or academic research and development, food scientists and technologists, materials scientists, mechanical engineers, industrial and systems engineers, toxicologists, analytical chemists, environmental scientists, regulatory officers, and other professionals who are concerned with advances in the development and applications of packaging.

Editor

Jay Singh
Industrial Technology
Cal Poly State University
San Luis Obispo, CA 93407, USA
Phone: 805-756-2129, Email: singhjapr@gmail.edu

Editorial Advisory Board

Rafael Auras
Michigan State University

Larry Baner
Nestle Purina Pet Care

Heather P. Batt
Clemson University

Vanee Chonhenchob
Kasetart University

Robert Clarke
Michigan State University

Lisa J. Mauer
Purdue University

Herbert Schueneman
San Jose State University

Tom Voss
Rochester Institute of Technology

Bruce Welt
University of Florida

Fritz Yambrach
San Jose State University

JOURNAL OF APPLIED PACKAGING RESEARCH—Published quarterly—
January, April, July and October by DEStech Publications, Inc., 439 North Duke Street,
Lancaster, PA 17602-4967.

This journal is recommended by The National Institute of Packaging Handling and
Logistics Engineers (www.niphle.org).

Indexed by Chemical Abstracts Service.

Indexed and abstracted by Pira International.

Subscriptions: Annual \$299 (Print), \$299 (Electronic) and \$324 (Print and Electronic).
Single copy price \$89.50. Foreign subscriptions add \$45 per year for postage.

(ISSN 1557-7244)



DEStech Publications, Inc.

439 North Duke Street, Lancaster, PA 17602-4967, U.S.A.

©Copyright by DEStech Publications, Inc. 2009—All Rights Reserved

C O N T E N T S

Student Contribution

- Packaging Trends for Bottled Water** 123
N. NOBLE, L. PAUL, C. MCMINIMEE, M. MALLETT and J. SINGH

Research

- Application of Finite Element Analysis to Predict the
Critical Top-Load of a Corrugated Box** 137
CHANGFENG GE

- New Pressure Sensitive Device to Measure and
Predict Package Drops** 149
S. PAUL SINGH, JAY SINGH and YOUNG PAEK

- Method for Measuring the Oxygen Transmission Rate of
Perforated Packaging Films** 161
AYMAN ABDELLATIEF and BRUCE A. WELT

Packaging Trends for Bottled Water

N. NOBLE¹, L. PAUL¹, C. McMINIMEE¹, M. MALLETT¹
and J. SINGH^{2,*}

¹Undergraduate Student, Packaging Program, Cal Poly State University,
San Luis Obispo, CA

²Associate Professor, Packaging Program, Cal Poly State University,
San Luis Obispo, CA

ABSTRACT: The *Journal of Applied Packaging Research* (JAPR) is an international forum for the dissemination of research papers, review articles, tutorials and news about innovative or emerging technologies for the packaging industry. In an effort to introduce research conducted by packaging students to the academics and industry professionals and to provide an outlet for these future stewards of the packaging industry to experience the world of publishing, JAPR, occasionally includes such work in its issues.

Bottled water is drinking water packaged generally in plastic bottles and regulated by national and local agencies. The Beverage Marketing Corporation defines the bottled water market segment as “retail PET, retail bulk, home and office delivery, vending, domestic sparkling and imports” but excluding “flavored and enhanced water”. Bottled water, with a fifth ranking amongst all beverage types consumed in the US at the beginning of this decade, has moved to the second slot, after carbonated soft drinks, in 2008. This has been accompanied by the bottled water category increasing its US market share from 4.7 billion gallons to 14.1 billion gallons and 15% of the beverage market share during this period. The following is a research paper submitted by a group of packaging students and their advisor at California Polytechnic State University, San Luis Obispo, California. This paper researches the trends observed in the bottled water industry globally and includes package designing palettes such as retail environment, shape, imagery, colors, and sustainability. This report also includes the results of a survey that helped the authors’ rank ten innovative bottled water solutions.

1.0 TRENDS

1.1 Retail Environment

BOTTLED WATER is among the most universally sold consumer products in the world. The retail venues for bottled water include

*Author to whom correspondence should be addressed. Email: jasingh@calpoly.edu



Figure 1. Varieties of bottled water.



Figure 2. Retail environment.

grocery stores, convenience stores, bulk stores, restaurants, and vending machines, among others. Point of sale displays are commonly used, although bottled water is typically displayed in cooler cases near other beverages such as energy drinks, sports drinks, and sodas.

1.2 Shape

The shape of a bottled water package is perhaps the most noticeable aspect. Although the standard bottle shape is still fairly prevalent, other forms such as pouches and cartons are gaining momentum. Additionally, the shape of the standard plastic bottle is being modified to include complex contours and swirls.

Response

The observed trends in bottled water package shapes are meant to catch the eye of the consumer. A sleek, contoured plastic bottle seems to be a highly desired component.



Figure 3. Shape.



Figure 4. Imagery: mountain scenes/nature scenes/water droplets.

1.3 Imagery: Mountain Scenes/Nature Scenes/Water Droplets

The mountain and nature scenes depicted on such well recognized water brands as Aquafina and Evian are a common and typical aspect of bottled water packages. Also commonly depicted are nature scenes and water droplets or snowflakes.

Response

The mountain and nature scenes are meant to convey a sense of freshness, purity, and coldness which many people associate with critical aspects of water. The operating assumption behind this nature related imagery is that many consumers associate the best water as coming from mountain springs and snow runoff.

1.4 Colors

Nearly every bottled water package we observed used some form of blue, in varying hues. Additional colors observed include white, yellow, and gold.



Figure 5. Colors.



Figure 6. Clear Panels.

Response

The prevalence of varying shades of blue in bottled water packaging serves to further convey the feeling of freshness and purity. Additionally, the blue color has a subliminal association with water for many consumers. Other colors such as white and gold are “soft” colors included to create an inviting tone.

1.5 Clear Panels

Another readily observable trend in bottled water packaging is the use of clear panels to give customers a glimpse of the water within. The sizes of these clear panels vary by brand.

Response

The use of clear panels is another attempt by the package designers to convey purity and to assure the customer that they are purchasing nothing but water. By being able to see through the product, the customer is more certain that there is nothing contaminating the water within.

1.6 Sustainability

Another observable trend within bottled water packaging is the use of more sustainable materials and the use of packaging designs which utilize less material. The use of flexible packaging such as pouches, as well as the use of new plastic bottle designs, reduces the required amount of plastic resin used per package. Additionally, the use of more sustainable materials such as paper (instead of or in conjunction with plastic) can be observed in many newer package designs.



Figure 7. Sustainability.

Response

The trend towards sustainability in water bottle packaging can be traced to the recent “green” movements of the current socio-economic climate, as well as the demonization of plastic in the media and increased concern over carbon footprint. With these more sustainable packages, consumers feel less guilty about purchasing bottled water because they feel that the packaging is less harmful to the environment.

2.0 TOP TEN BOTTLED WATER PACKAGES

In order to further discover trends in the water bottle market, the team posted a survey online that was taken by 108 people in the San Luis Obispo County of California, comprising of 71% female and 29% male respondents. 68% of these respondents were between the ages of 21–25 and 24% were between the ages of 15 to 20. The purchasing habits towards bottled water are described in Figure 8.

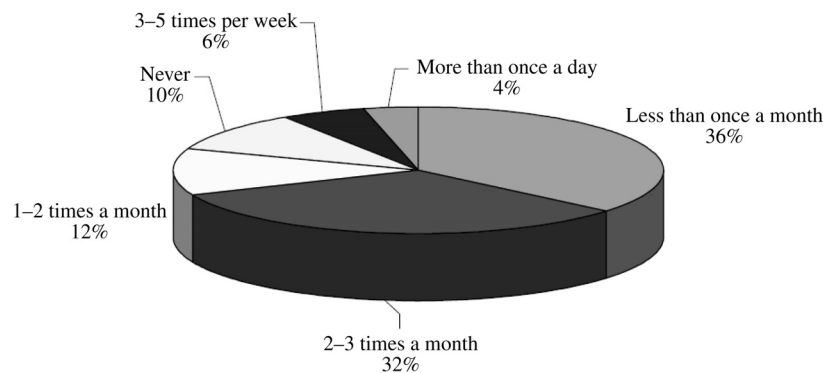


Figure 8. The purchasing habits towards bottled water.

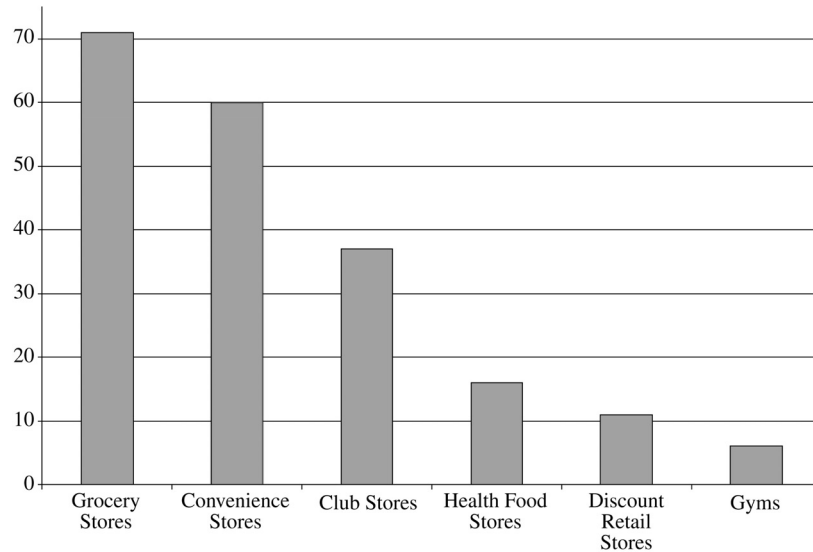


Figure 9. Locations where the respondents most commonly purchased bottled water.

Figure 9 shows the responses to locations where the respondents most commonly purchased bottled water.

The respondents were also asked to rank 15 different kinds of packages in the order of preference and the top ten packages are listed below.

1. Nao

Nao water bottles are made by the Jumeirah Hotel Group and designed by Fig Tree. This package is used in luxury hotels by the Jumeirah Hotel



Figure 10. Nao water bottles.

Group. The bottles are made of glass and have a sleek, new age look which appeals to the higher class. The process used to make these bottles is the press and blow process. Because these bottles are found in hotels, they do not get any bigger than about 12 oz. The target market consists of higher class, middle age people who spend a considerable time traveling because these are mostly found in luxury hotels.

2. Tap'd NY

Tap'd NY is a new brand of bottled water where the contents are nothing more than New York City tap water! They don't even hide it, in fact, it's part of their brand ethos. The design of the bottle is simple and transparent, and features the pipelines reminiscent of the layered NYC skylines. The colors were chosen to be orange and blue, the same as those of the Flag of the City of New York. Credits for the concept and design are shared between "many people", according to Craig Zucker of Tapped Drinks. This is manufactured by, Tap'd New York, and is made from PET. The bottle is injection blow molded, offered in 10, 16 and 20 oz bottles. It is targeted to middle and upper middle class people of New York, ages 14 and up, and is sold in convenience and grocery stores, and by street vendors in New York. It is unique because Tap'dNY is bottled water for the new age: an honest and local alternative for all New Yorkers. They purify and bottle New York City's famous tap water, leaving out the malarkey and long distance journey included in other bottled waters.



Figure 11. Tap'd NY.



Figure 12. 1 litre™.

3. 1 litre™

1 litre™ has combined the elements of exceptional design and uncompromising taste to create a unique, stand-alone product with international appeal. The clean, crisp taste coupled with the innovative and uber-chic design, make 1 litre™ a natural complement to finest restaurants, luxury hotels, resorts, spas, casinos, meeting rooms etc. around the globe. It is manufactured by 1 litre bottle company, and is made from PET, injection blow molded, and is offered in half and full liter sizes. It is targeted toward upper middle class to upper class people, ages 14 and up. It is sold at the finest restaurants, luxury hotels, resorts, spas, casinos, meeting rooms etc. around the globe. It is unique because it is the first bottle in the world to feature an integrated cup. The proprietary design has been acknowledged as the most functional, sophisticated and visually appealing bottle on the market.

4. Aquafina

Aquafina is a product by Pepsi Co. that is marketed internationally. This bottled water is a standard for convenience and portability. The custom shape of the bottle is recognizable and acts as a branding tool for Aquafina. The bottle is made from PET and is injection blow molded into a proprietary custom mold. The water bottle is marketed to a wide target market focusing on middle class from the ages of 18+. This product can be purchased at most general market stores including grocery stores, convenience stores, and restaurants. This bottle was designed as an eco-friendly bottle. It reduces the amount of plastic used by 50 percent. The Aquafina bottle was the industry's lightest water bottle at the time of this study.



Figure 13. Aquafina.

5. Malmberg

Malmberg water is a fine mineral water collected from an artesian spring in southern Sweden. It is known for its low salt content, distinct intensity, and neutral mineral tone with a hint of carbonation. It comes in a few different bottles that can be made of glass or plastic. The bottles vary in sizes and include 25 oz., 16 oz., and 11 oz.

The bottles are manufactured in Sweden and are made using different processes depending on the material of the bottle. The glass bottles are made using the narrow neck stretch and blow process and the plastic bottles are made using the injection blow molding process. This product is targeted towards the health conscious naturalist that is looking for a refreshing sip of natural spring water. Something unique about this water is the location from which it comes and the hint of carbonation they add to it, giving the buyer a slight tingle upon consumption. This drink is sold primarily in Sweden but can be ordered through an online store.



Figure 14. Malmberg.



Figure 15. 360 Paper Bottle.

6. 360 Paper Bottle

The 360 Paper Bottle is an innovative new product designed and manufactured by Brand Image. The product is a single serve paper water bottle with an innovative cap feature unlike anything currently on the market. Marketing appeal for this product is the sustainable nature of the materials, the recyclability of the container after use, and the sleek modern design. The product is manufactured by sealing two halves of sheet stock to attain the final shape. The product is currently unavailable for retail purchase in the United States, but would eventually be featured in health-food stores, convenience stores, and grocery stores. The target market is environmentally conscious adults.

7. KOR ONE Hydration Vessel

This thoughtful and attractive bottle manufactured by KOR ONE, was



Figure 16. KOR ONE Hydration Vessel.

designed with the intention of encouraging consumers to reuse water bottles. The bottle is made with PET and is created by extrusion blow molding. The target audience is active individuals between the ages of 18-50. The bottle was designed by One of Eastman and RKS design. The major goal of the bottle is function and convenience. The bottle offers the ability to drink with one hand with the hinge snap cap. It has a wide mouth cap for easy fill. The mouth also offers enough room to fill the bottle with ice. This unique and innovative bottle design combines function and aesthetic appeal.

8. Another Bloody Water

Another Bloody Water is natural spring water that comes from the Victorian Alps. It is sourced from an aquifer 70 meters below the surface, and is separate from ground water, like rivers and creeks so it does not take water away from the farmers. The water is possibly hundreds of years old and is encased in rock granite, and its levels of the aquifer are constantly checked and has been confirmed to be renewable.

The bottle shape is a proprietary design and unique to Another Bloody Water. It is manufactured in Australia, made from PET, injection blow molded, and offered in a variety of sizes—most popular are 12, 16 and 24 oz sizes. The target market segment is middle to upper middle class people, ages 18–40. It is sold at general and convenience stores in and around Australia. The unique marketing features for this product is that the name and branding is blunt and to the point. The text is printed directly on the bottle for added visual appeal.



Figure 17. Another Bloody Water.



Figure 18. Malmberg.

9. Boxed Water Is Better

Boxed Water Is Better is a manufacturer of boxed water out of Michigan. The product features a 100% recyclable paper carton instead of the traditional bottle. The recyclability of the container and the fact that each carton is made using sustainable materials provide the main marketability for this product. Form, fill and seal concept is used for manufacture of the packages and filling of the product within. The product is available in 20 oz and 1 liter sizes and is sold at convenience stores and grocery stores. The target market for Boxed Water Is Better is environmentally conscious individuals of all adult age ranges.

10. Pique

Pique water bottles are “The world’s first water that infuses a special



Figure 19. Pique.

blend of ingredients that reinvigorate tired minds and bodies with much needed vitamins and minerals.” These eye catching bottles are designed by David Fung. They are made of glass using the narrow neck press and blow process. The target market for these bottles is made up of people who are looking for that extra energy boost but have a little more money to spend because of the glass bottles. Because of the appearance, they are targeting a more mature crowd instead of the young, edgy energy drink seekers. A unique marketing feature of these bottles is that they are made of glass. That gives the consumer a feeling of value and they feel like they are purchasing a high class product.

Application of Finite Element Analysis to Predict the Critical Top-Load of a Corrugated Box

CHANGFENG GE

¹*Rochester Institute of Technology, 78 Lomb Memorial Drive,
Rochester, NY 14623, USA*

ABSTRACT: Most nonlinear finite element analysis (FEA) studies for a single-wall corrugated board assume that the board is a three-layer laminated orthotropic plate. As inputs to FEA software, the mechanical properties of the board are usually calculated from experimentally obtained properties of single layers. This study used corrugated board in a cross-machine direction as a pseudo-isotropic component for experimental evaluation. The measured board properties were then input into FEA software to model a corrugated box. A load curve was created in FEA software to simulate box compression testing. The FEA-predicted critical top-load was compared to experimental results of regular slotted containers (FEFCO 0201) and analytical estimations based on the McKee formula.

INTRODUCTION

CORRUGATED BOARD BOX is the most common form of transport packaging for all industries. There are two ways to predict the critical top-load of a regular slotted corrugated box: the analytical method and the numerical method. The most representative analytical method is the McKee formula, which has been effectively used by the packaging industry for the last 45 years. According to McKee, the top-to-bottom compression strength of an RSC (regular slotted container)-style corrugated box can be estimated using the following formula:

$$P \text{ (lb)} = 5.87 \times ECT \times \sqrt{T \times BP}$$

where P is the critical top-load; ECT is the edge crush test value (lb/in); T is the board thickness (in); and BP is the box internal perim-

*Author to whom correspondence should be addressed. Email: cfgmet@rit.edu

eter ($2 \text{ Length} + 2 \text{ Width}$) of the box (in). All parameters are in imperial units.

Since the 1990s researchers have been using finite element analysis (FEA) to analyze the compression strength of corrugated board panels and boxes as well. The finite element method was first introduced by Pommier in 1991 to develop a linear elastic model for a corrugated box using the SYSTUS system [2]. The system inputs were mainly the Young's modulus of the paper types and the structural elements of the box (thickness and dimensions). The research compared the theoretical and experimental critical loads and the limits of the SYSTUS code. Gilchrist [3] created an FEA nonlinear-elastic model for C-flute corrugated board based on ABAQUS. The FEA model correlates reasonably well to the analogous measurements based on the results of four-point bending testing. Also based on ABAQUS, Beldie [4] developed an FEA model for corrugated board and boxes to compare the actual compression test results for corrugated board and boxes. The FEA model for corrugated board showed good agreement with the experimental results. However, the box model and box compression test results in this study did not statistically agree.

Most of the aforementioned nonlinear FEA models were based on an assumption that corrugated board was a classical laminated orthotropic plate. The development of the above FEA model approach started by obtaining the mechanical properties of single layers through measurement and summed these layer properties to board parameters. The calculated board properties were then input into FEA software. The theoretical combination from single layer properties to board properties led to a reasonable matching between the FEA model and measurements for a piece of corrugated board, but it appeared less effective for predicting the compression strength of corrugated boxes.

Instead of measuring the properties of single paper layers, the present study used corrugated board as an isotropic component for experimental preparation. Three-point bending test and edge compression tests were performed to evaluate the materials properties of the corrugated board. Then, the study attempted to create a load curve in the FEA software to simulate the box compression testing process. Under this simulated loading process, a nonlinear FEA model was developed to predict the critical top-load of corrugated board boxes. Both box compression testing and analytical estimation using the McKee formula were carried out to corroborate the FEA predictions.

MEASUREMENTS

In order to perform an FEA simulation, three mechanical properties need to be measured: shear modulus, elastic modulus and Poisson ratio. The materials tested in this study were 14.5 kgf ECT C- flute corrugated board. The thickness of the board was 4.06 mm. All measurements took place in ambient environment (23°C and 40% RH) on an MTS universal testing machine (MTS Systems Corporation, Eden Prairie, MN, USA) equipped with compression anvils.

Shear Modulus of the Pseudo-isotropic Corrugated Board

Shear modulus was determined by the three-point bending test (Figure 1). The corrugated box buckles both in cross-machine direction and machine direction when it is compressed in the- cross-machine direction. Therefore, bending strength in both the cross direction (CD) and machine direction (MD) of the corrugated board was measured. The dimension of the sample was 50.8 mm × 152.4 mm as suggested by Gilchrist [3].

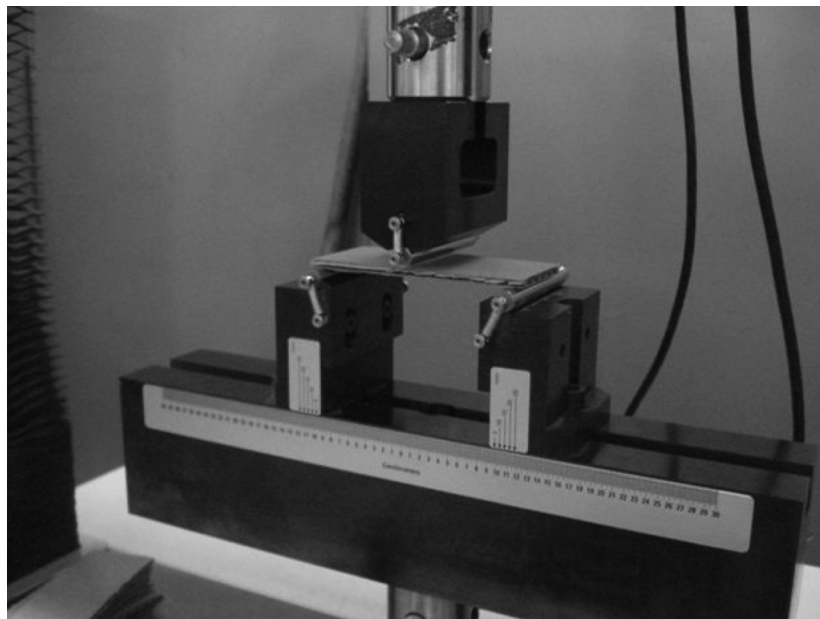


Figure 1. Three- point bending testing in cross-machine direction.

Table 1. Three (3)-point Bending Testing Results in the Cross-machine Direction.

Specimen #	Width (mm)	Thickness (mm)	Peak Load (kg)	Flexural Strength (kPa)	Shear Modulus (kPa)
1	50.8	4.22	1.70	28.4×10^2	87.7×10^4
2	50.8	4.22	3.10	52.0×10^2	86.2×10^4
3	50.8	4.24	2.91	48.2×10^2	87.4×10^4
4	50.8	4.24	1.78	29.4×10^2	89.9×10^4
5	50.8	4.24	3.05	50.3×10^2	91.8×10^4
Mean	50.8	4.24	2.51	41.7×10^2	88.6×10^4
Std. Dev.	0.00	1.27×10^{-2}	7.06×10^{-1}	11.7×10^2	22.1×10^3

Tables 1 and 2 summarize the basic mechanical properties from the bending test. The averaged shear modulus in the cross-machine direction, G_c , was 88.6×10^4 kPa. The averaged shear modulus in the machine direction, G_m , was 70.9×10^4 kPa. Therefore, the shear modulus G of the pseudo-isotropic corrugated board was approximately 79.75×10^4 kPa, an averaged value from G_c and G_m .

Young's Modulus for Pseudo-isotropic Corrugated Board

In order to simulate actual compression testing, the elastic modulus was measured with an edge compression test in accordance to TAPPI standard T811. Samples were cut into 50.8 mm \times 50.8 mm for testing and were positioned such that the compression direction was the same as the cross-machine direction or flute direction. Table 3 shows the measured mechanical properties when the board was compressed in the

Table 2. Three (3)-point Bending Testing Results in the Machine Direction.

Specimen #	Width (mm)	Thickness (mm)	Peak Load (kg)	Flexural Strength (kPa)	Shear Modulus (kPa)
1	50.8	4.19	7.85×10^{-1}	13.8×10^2	69.2×10^4
2	50.8	4.27	1.83	29.5×10^2	80.0×10^4
3	50.8	4.17	1.89	32.9×10^2	73.5×10^4
4	50.8	4.22	1.93	32.2×10^2	71.9×10^4
5	50.8	4.24	8.12×10^{-1}	13.4×10^2	68.7×10^4
Mean	50.8	4.22	1.45	24.3×10^2	70.9×10^4
Std. Dev.	0	5.08×10^{-3}	9.03×10^{-1}	9.90×10^2	19.9×10^3

Table 3. Edge Compression Test Results.

Specimen #	Width (mm)	Thickness (mm)	Peak Load (kg)	Peak Stress (mm)	Elastic Modulus (mm)
1	50.8	4.22	22.6	13.8×10^2	3.84×10^4
2	50.8	4.22	14.1	6.89×10^2	3.60×10^4
3	50.8	4.22	23.9	13.8×10^2	3.66×10^4
4	50.8	4.19	20.7	6.89×10^2	3.58×10^4
5	50.8	4.19	11.1	6.89×10^2	9.50×10^4
Mean	50.8	4.21	18.5	9.65×10^2	3.12×10^4
Std. Dev.	0	1.73	9.06	5.17×10^2	1.68×10^4

cross direction. The averaged elastic modulus of the pseudo-isotropic board, E , was found to be 3.12×10^4 kPa.

Poisson Ratio of the Pseudo-isotropic Corrugated Board

Poisson ratio of an isotropic material can be defined as follows:

$$\nu = - \frac{\varepsilon_{trans}}{\varepsilon_{axial}} \quad (2)$$

where,

ε_{trans} is transverse strain and ε_{axial} is axial strain.

Poisson ration ν can also be expressed in the following formula:

$$\nu = \left(\frac{E}{2G} \right) - 1 \quad (3)$$

where,

E is the elastic modulus and G is the shear modulus.

Unlike a metal or polymer sample, corrugated board does not have a clear plastic deformation process when a sample undergoes compression. Corrugated board tends to break suddenly at the jaw location or buckle in the middle of the sample when compression force is applied. Therefore, the Poisson ratio based on Equation (2) was difficult to measure due to the difficulty of getting the strain ε in a very short time.

The Equation (3) was used in this study to calculate the Poisson ratio based on results of the averaged elastic modulus $E = 3.12 \times 10^4$ kPa and shear modulus $G = 79.75 \times 10^4$ kPa:

$$\nu = \left(\frac{E}{2G} \right) - 1 = \left(\frac{31200}{2 \times 797500} \right) - 1 = -9.80 \times 10^{-1} \quad (4)$$

Materials with a negative Poisson ratio (NPR) are uncommon. When a NPR material is compressed, the material compresses instead of expanding. The negative Poisson ratio calculated from Equation (4) reflects a moment when the corrugated board starts buckling. When the board was crushed to achieve buckling during the edge compression test, the board at the buckling point shrank to a thin layer in the transverse direction from its original thickness. This board buckling is correlated to the buckling of a corrugated box.

FINITE ELEMENT ANALYSIS

The software ALGOR- FEMPRO V22 (Figure 2) was used for performing finite element analysis. The corrugated box used for modeling was a flapless shelled box. The box model was made of a 4.06 mm thick plate to simulate the C-flute corrugated board. The internal dimensions of the box model were 305 mm × 305 mm × 203 mm. The mesh size of the box model was set to 40%, which corresponds to a total of 3760 finite elements for the entire box. The box model was defined to have a large and non linear displacement during the loading process. In order to simulate physical compression testing, the bottom surface boundary condition of the box was set as fixed. A load curve from 0 to 700 kg was created to apply a uniform loading onto the top surface of the box model at a rate of 21.8 kg/second.

Table 4 illustrates the maximum von Mises stresses and the corresponding displacements both in the center and top middle of the side panel of the box during a 16-second loading process. The maximum von Mises stresses are shown in Figure 3 where the maximum von Mises stresses are highlighted in red. The center part of the box collapsed shortly after the load applied reached 65.3 kg. When the load on the top surface increased to 327 kg, the von Mises stress and displacement on the top middle of the side panels reached a maximum of 19.8×10^3 kPa and 3.94 mm. A further increase of the load resulted in panel buckling, where the von Mises stresses and displacement became zero. 327 kg was the predicted value as the critical top-load representing buckling of the box or the compression strength of the corrugated box.

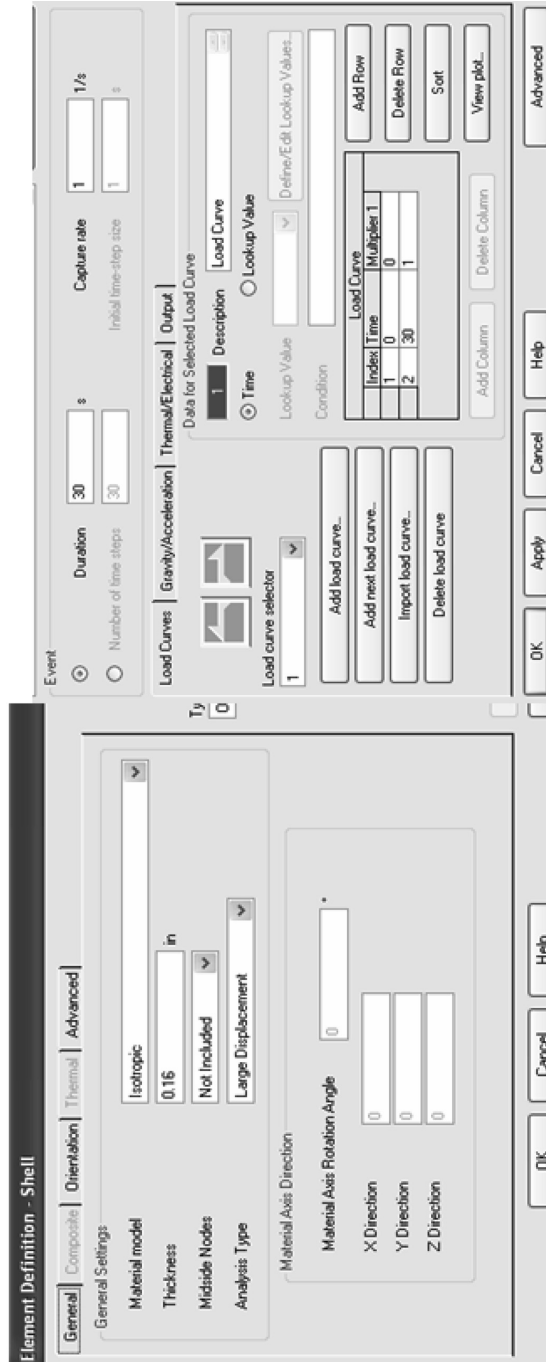


Figure 2. Schematic diagram of the FEA set up.

Table 4. Load, Maximum von Mises Stress and the Corresponding Displacement.

Applied Time (s)	Applied Load (kg)	Maximum Von Mises Stress in the Top Middle of the Side Panel (kPa)	Corresponding Displacement in the Top Middle of the Side Panel (mm)	Maximum Von Mises Stress in the Center on the Top Face (kPa)	Corresponding Displacement in the Center on the Top Face (mm)
0	0.00	0.00	0	0.00	0.000
1	21.8	1.26×10^2	2.03×10^{-1}	17.9	1.22
2	43.5	25.4×10^2	4.32×10^{-1}	36.1	2.44
3	65.3	38.2×10^2	6.60×10^{-1}	0	0
4	87.1	51.2×10^2	9.89×10^{-1}		
5	109	64.2×10^2	1.14		
6	131	77.4×10^2	1.37		
7	152	90.5×10^2	1.65		
8	174	10.4×10^3	1.91		
9	196	11.7×10^3	2.16		
10	218	13.1×10^3	2.44		
11	240	14.4×10^3	2.74		
12	261	15.8×10^3	3.02		
13	283	17.1×10^3	3.33		
14	305	18.4×10^3	3.63		
15	327	19.8×10^3	3.94		
16	348	0	0		

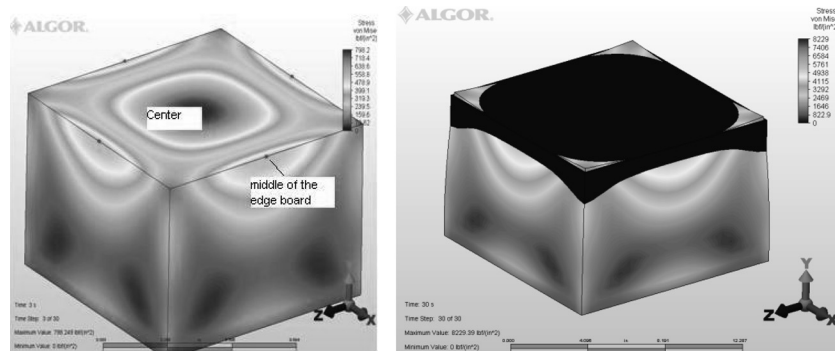


Figure 3. FEA model at the beginning of the loading (left) and the final step (right).

Figure 3 shows two areas on the box model having stress concentration after the load was applied. They are the center part on the top face and the top middle part of the four side panels (Figure 3). The left figure is the FEA model at the beginning of the loading and the right figure demonstrates the box collapse under a uniformly applied load. The Von Mises stresses in Figure 3 are represented in different colors; dark blue represents zero stress and red represents the highest stress. (These are lighter and darker areas on the black and white version.)

BOX COMPRESSION TEST

Boxes used for compression testing consisted of 5 samples with an internal dimension of 305 mm × 305 mm × 203 mm. Regular slotted containers (RSC, FEFCO 0201) were designed using ArtiosCAD software and cut using a M series CAD cutting table (Data Technology, MA, USA).

ASTM D 642 standards were followed in conducting the compression testing. A Lansmont Model 125-15 (Lansmont, Monterey, CA, USA) compression tester was used for the testing. The compression testing machine had a 22.7 kg preload with a stop force of 6.58×10^3 kg. The test speed used was 25.4 mm/min. Auto sample and auto log on test comple-

Table 5. Box Compression Testing (BCT) Data.

Sample #	1	2	3	4	5	Mean	Std. Dev.
Max. Strength (kg)	345	357	357	368	342	354	9.34
Displacement (mm)	11.2	10.4	10.7	9.14	10.2	10.3	7.62×10^{-1}

tions were turned on. The compression machine automatically stopped the test when a -12.7 mm deflection of the box occurred or a -10% of maximum yield appeared during the compression test.

McKEE FORMULA ESTIMATION

In order to calculate the critical top-load estimated by the McKee formula in imperial units, edge crush testing (ECT) was carried out to obtain the ECT value. After averaging 5 samples, the ECT value was equated to 37 lbs./in. Together with the board thickness ($T = 0.16$ in.) and the box perimeter ($BP = 48$ in.), the measured ECT = 37 lb/in were placed into Equation (1) for estimating the critical top-load:

$$P \text{ (lb)} = 5.87 \times 37 \times \sqrt{0.16 \times 48} = 602 \text{ (lbs)}$$

The estimated critical top-load was 273 kg (602 lbs).

RESULTS COMPARISON

Table 6 provides a comparison of the critical top-load among the FEA prediction, McKee Formula and the box compression testing (BCT). In comparison to the physical testing result, the FEA predicted result was 7.6% lower and the McKee estimation was 22.8% lower. The FEA prediction showed agreement with the BCT results as compared to McKee's equation. The samples for mechanical properties measurement were from the standard supplied samples with a dimension of 254 mm \times 254 mm. The samples for compression testing were taken from a lot that was shipped on a pallet. Different batches of the samples could have affected the accuracy of the FEA prediction.

Table 6. Comparison Between FEA Prediction, McKee Calculation and Actual Testing.

Evaluation Methods	The Critical Top-load (kg)	The Correspondent Displacement (mm)
FEA prediction	327	3.94
Box compression testing (BCT)	354	103
Estimation from McKee formula	273	N.A.

CONCLUSION

This study has proposed a practical concept regarding corrugated board as a pseudo isotropic component for FEA simulation. The method makes it possible to predict the failure mode of a corrugated box based on FEA stress concentration. The research proved the hypothesis that the tested board parameters give a more direct correlation to box compression strength than calculated inputs in FEA.

Creating a load curve in FEA software to simulate an actual compression test is possible. The critical top-load of a corrugated board box in this research was identified as the load that caused the maximum von Mises stress in the top middle of side panels of the box.

The study experimentally determined the shear modulus both in cross-machine direction and machine direction and the elastic modulus of corrugated board in cross-machine direction and then calculated the Poisson rate based on the measured modulus.

Both the McKee formula and the FEA prediction took a similar approach: predicting the corrugated box strength through measuring properties of corrugated board. Applying FEA to predict the box strength showed better accuracy than the McKee formula in this study due to advantages of finite element analysis.

REFERENCES

1. R.C. McKee, J.W. Gander and J.R. Wachuta, Compression Strength Formula for corrugated board paper board packaging, *Performance and Evaluation of Shipping Containers*, compiled and edited by George G. Maltenfort, 1989, Jelmar Publishing Co., Inc. P62–73.
2. J.C. Pommier, J. Poustis, E. Fourcade and P. Mourier, Determination of the critical load of a corrugated box subjected to a vertical compression by finite element methods, *Proceedings of the 1991 International Paper Physics Conference, Kona, Hi*, P437–447.
3. A.C. Gilchrist, J.C. Suling and T.J. Urbanik, Nonlinear Finite Modeling of corrugated board, *Mechanics of Cellulosic Materials*, AMD-Vol. 231/MD-Vol.85, 1999, P101–106.
4. Liliana Beldie, Goran Sanberg and Lars Sandberg, Paperboard packages expose to static loads-finite element modeling and experiments, *Packaging Technology and Science*, Vol. 14, 2001, Pages 171–178.
5. Rami Haj-Ali, Joonho Choi, Bo-Siou Wei, Roman Popil, Michael Schaepe, Redefined nonlinear finite element models for corrugated boards, *Composite Structure* Vol. 87, 2009, page 321–333.
6. Optimum design of corrugated board under buckling constraints, T. Daxner, T. Flatscher and R.G. Rammerstofer, *7th World conference on structural and multidisciplinary optimization*, Coex Soul, 21-May-25 May, 2007.
7. T.J. Urbanik, Review of buckling mode and geometry effect on post buckling strength of corrugated containers, PVP Vol 343, *Development, validation and application of inelastic methods of structural analysis and design*, 1996.

New Pressure Sensitive Device to Measure and Predict Package Drops

S. PAUL SINGH^{1,*}, JAY SINGH² and YOUNG PAEK³

¹*Professor, School of Packaging, Michigan State University, East Lansing, Michigan, USA*

²*Associate Professor, Industrial Technology, Cal Poly State University, San Luis Obispo, CA*

³*Graduate Assistant, School of Packaging, Michigan State University, East Lansing, Michigan, USA*

ABSTRACT: Pressurex[®], a tactile pressure sensor film which is manufactured by Sensor Product Inc. (East Hanova, NJ, USA), is one of the emerging materials that is convenient for measurements of the strength of pressure and pressure distribution profile between two contacting surfaces without any instrumentation. It immediately reveals impact distribution and magnitude based on intensity and dispersion of color. The intensity of this color is proportional to the amount of force applied allowing the user to actually quantify the stress characteristics across the impact surface. The objective of this paper was to examine free fall drop test results using six different ranges of sensor films with two cushion materials as backing (plastic corrugated and foamed polystyrene sheets). Throughout this study, the dispersion of force and pressure strength through the different free fall drop heights was evaluated using these materials. The best film and cushion material to predict drop height was selected using visual inspection of the imprinted surface based on the magnitude of the color and intensity on the film. A correlation was developed based on the area and diameter of the imprinted surface.

1.0 INTRODUCTION

IN the journey through the supply chain, all packages are expected to protect the product from various static and dynamic hazards they experience such as drops, impacts, vibration, compression and climatic. Damage during handling (loading, unloading and sorting) is commonly observed. Thus for a safe product delivery a functional and efficient cushioning material that can isolate most of the forces from reaching the product is usually desired. In addition to both the federal and state re-

*Author to whom correspondence should be addressed. Email: singh@msu.edu

quirements there are several trade associations and professional organizations that through their membership develop packaging test methods that manufacturers can use for a given application. The associations and organizations most involved in developing the distribution packaging standards are International Standards Organization (ISO), American Society of Testing and Materials International (ASTM) and International Safe Transit Association (ISTA). Although these standards are adequate in replicating the distribution hazards, they are unable to provide visual evidence of the amount of pressure experienced, during say a drop, between the product and the package.

Pressurex[®], a tactile pressure sensor film which is manufactured by Sensor Products Inc. (East Hanova, NJ, USA), provides a convenient tool to measure the strength of the pressure and pressure distribution profile between two contacting surfaces without any instrumentation. It immediately reveals impact distribution and magnitude by intensity and dispersion of color which is proportional to the amount of force applied allowing the user to actually quantify the stress characteristics across the surface [1]. That is to say, greater pressure has higher intensity imprint on the film. While conventional lab test instruments commonly used, such as triaxial accelerometers, are expensive and difficult to measure impact profile during transportation, these sensor films can easily be inserted between product and package to determine the impact levels during an impact, economically. There are no studies done to evaluate performance and accuracy of sensor films as an alternative of the conventional impact and pressure test method for replication of impacts experienced by packages in distribution.

For this study six different types of pressure sensitive films; Ultra Low, Super Low, Low, Medium, High, and Super High were obtained from Sensor Products Inc. These films were backed with two different types of materials and placed under spherical shaped weights of 3.6 kg and 6.8 kg (8 lbs and 15 lbs) and approximately 200 mm (7.90 in) in diameter. The setup was then placed in corrugated boxes. The test packages were then allowed to fall freely from different heights. Observations were then made on the film for distribution and magnitude of the force experienced.

The objective of this research was to examine free fall drop test results using six different types of pressure films with two cushion materials, corrugated plastic and foamed polystyrene sheets. Throughout this study, the dispersion of force and pressure strengths through the differ-

ent free fall drop heights was evaluated using these materials. The best film and cushion material to predict drop height was selected using visual inspection of the imprinted surface based on the magnitude of the color and intensity on the film. A correlation was then developed based on the area and diameter of the imprinted surface.

2.0 EXPERIMENTAL DESIGN AND MATERIALS

2.1 Pressure Indicating Sensor Films

Sensor Product Incorporated's tactile pressure indicating sensor film (Pressurex[®]) is marketed as a unique, affordable and easy to use tool for revealing the distribution and magnitude of pressure between any contacting, mating or impacting surfaces [1]. The materials were initially developed for the National Aeronautical and Space Administration (NASA) for aerospace applications. Pressurex[®] is a mylar film containing a layer of microcapsules that rupture producing an instantaneous and permanent high resolution "topographical" image of pressure variation across a contact area upon the application of force [1].

Pressurex[®] is extremely thin (0.10, 0.20 and 0.51 mm or 4, 8 and 20 mils) and provides a suitable alternative for strain gauges and load cells. It can function between 5°C to 35°C (41°F to 95°F) and 20% to 90% relative humidity ranges. With a shelf life of 2 years, Pressurex[®] provides $\pm 10\%$ visual accuracy and $\pm 2\%$ accuracy utilizing optional optical measurement systems [1]. Application areas for this product include aerospace, automotive, electronics, medical, packaging, plastics and printing/papermaking. Figure 1 shows the structure and functionality of this material.

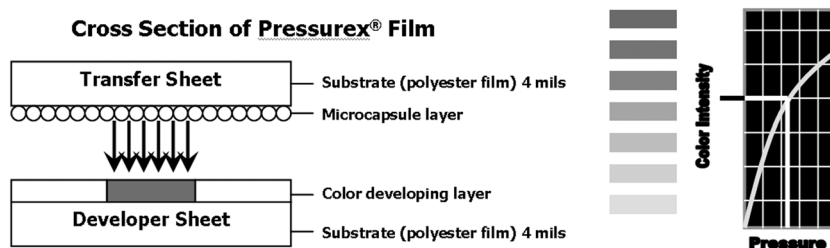


Figure 1. Cross section of Pressurex[®] film and color intensity scale.

Table 1. Sensitivities of Various Pressurex® Films.

Film Type	Pressure Range
Ultra Low	28–85 psi (2–6 kg/cm ²)
Super Low	70–350 psi (5–25 kg/cm ²)
Low	350–1,400 psi (25–100 kg/cm ²)
Medium	1400–7,100 psi (100–500 kg/cm ²)
High	7100–18,500 psi (500–1,300 kg/cm ²)
Super High	14400–43,200 psi (1,012–3,037 kg/cm ²)

This product is available for a wide range of pressures (1.97–3,037.26 kgf/cm² or 28–43,200 psi) as shown in Table 1.

2.2 Cushioned Backing Material

The two types of cushioned backing materials used in the study were single wall, profile extruded polypropylene corrugated sheets weighing approximately 1.07 kg/m² (220 lbs/1,000 ft²) and extruded expanded polystyrene foam panels measuring 7 mm (0.28 in) in thickness.

2.3 Corrugated Boxes

Regular slotted containers (RSC) made with single-wall C-flute corrugated board were used in this study. The dimension of the box was 219 x 219 x 241 mm (8.63 x 8.63 x 9.5 in).

2.4 Weighted Spheres

For the test product, two different weighted spheres (3.6 and 6.8 kg) measuring 200 mm (7.9 in) in diameter were used. The spherical weights were selected because of their complex shape (sphere versus cube) and because it produced a shape dependent imprint as a function of impact energy (drop height).

2.5 Test Setup

Two types of cushioning materials used as backing for the Pressurex® film were plastic corrugated sheets and expanded polystyrene (EPS) foam sheets. Both were approximately 7 mm (0.28 in) thick. The different types of pressure sensitive film were applied to the backing material.

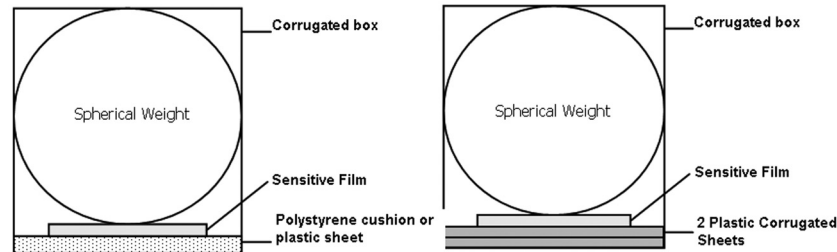


Figure 2. Test package configurations.

The spherical weight was placed on the pressure sensitive film and placed inside a single wall regular slotted container (RSC) style box. The test package arrangement is shown in Figure 2. The test packages were then subjected to drop heights from expected drop levels as recommended by ASTM D4169 [2].

2.6 Test Conditions

All samples were conditioned at a temperature of 23°C (73.4°F) and 50% relative humidity for at least 24 hours in accordance with the atmospheric conditioning, which is recommended in ASTM D 4332 [3].

2.7 Test Procedure

Eighteen test boxes (three replicates for each of the six types of pressure sensitive films) were made from single-wall C-flute corrugated board to perform drop tests using the pressure sensitive films to observe correlation between the size of the imprint and drop height. The main objective of the study was to determine if this film can be used as a sensor to determine drop height levels inside packages based on the color and size of imprint. The correlation was based on the major diameter of the imprint or the total imprint area versus the drop height for the various combinations. Since the package weighed less than 9 kg (20 lbs), drop heights between 0.45 to 1.21 m (18 and 48 inches) were selected as recommended in ASTM D4169 for the three assurance level extremes [2]. Testing was conducted in the following three phases:

1. During the initial phase to evaluate the optimum combination that provided the best visual results, drop heights of 0.61, 0.76 and 0.91 m

(24, 30 and 36 in) were used for all six grades of sensor films with the two types of backing materials. The imprints were visually examined.

2. For phase two, drop heights of 0.45, 0.66, 0.86 and 1.22 m (18, 26, 34, and 48 in) were used to further narrow down the qualification for the optimum combinations using the best results from phase one.
3. Having found the best combinations from phase two testing, further testing was conducted using the optimum combinations of sensor film, backing material and spherical weights. Drop heights of 0.61, 0.76 and 0.91 m (24, 30 and 36 in) were used to quantify the pressure imprints on the sensor films and the derivation of the regression relationships to predict drop heights.

3.0 RESULTS AND DISCUSSION

3.1 Phase I: Comparison of the Performance of Different Films

Using the two different packages (Figure 2), six different pressure sensitive films were tested to select the most adequate film to represent commonly occurring package drop heights. The drop heights used were 0.61, 0.76 and 0.91 m (24, 30 and 36 in) for the initial phase. The results for the first phase are shown in Figures 3, 4, and 5.

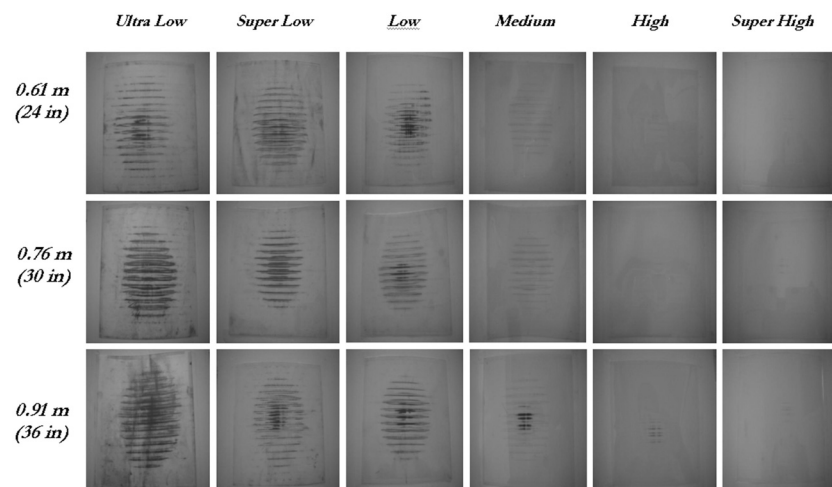


Figure 3. Results of drops using 3.6 kg (8 lb) spherical weight and plastic corrugated backing.

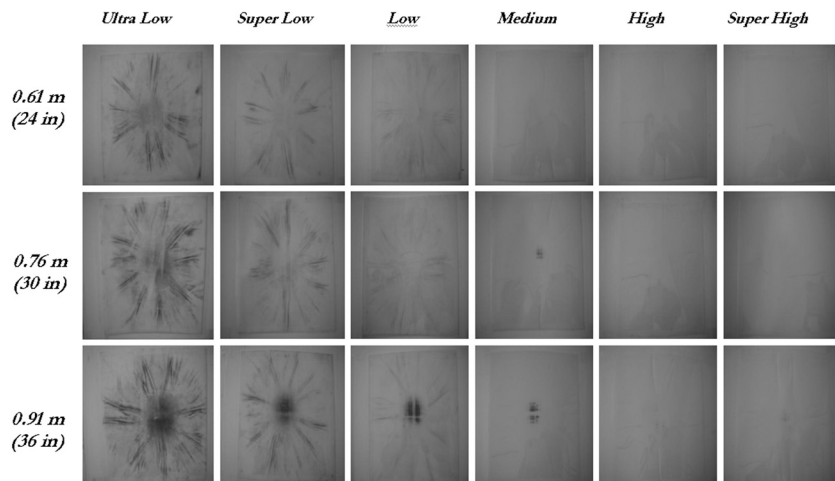


Figure 4. Results of drops using 3.6 kg (8 lb) spherical weight and EPS backing.

As shown in the results in Figures 3 through 6, Ultra Low and Super Low sensor films with 6.8 kg (15 lb) and soft backing materials showed obvious differences in the intensity of color for the pressure marks on the film as a function of the drop height. On the other hand, there were less significant differences between the intensity on the imprint when Low, Medium, High, Super high films were used. In the case of High

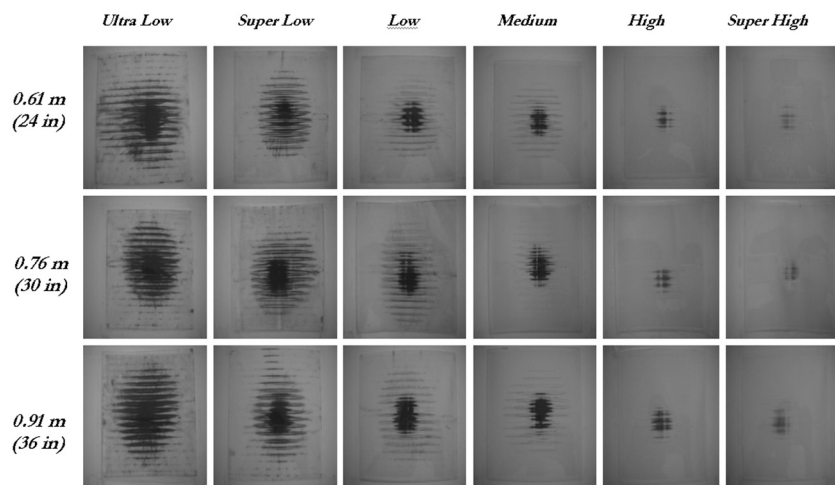


Figure 5. Results of drops using 6.8 kg (15 lb) spherical weight and plastic corrugated backing.

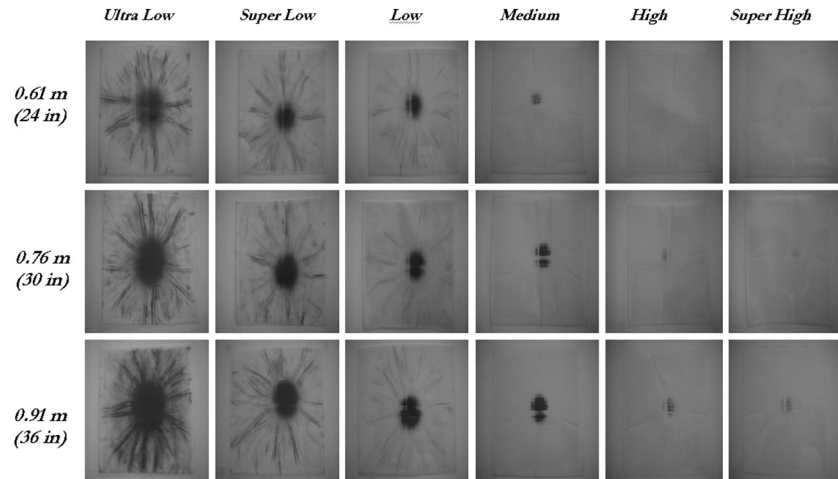


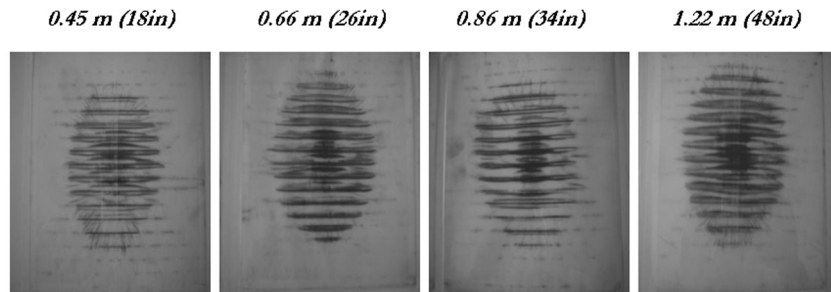
Figure 6. Results of drops using 6.8 kg (15 lb) spherical weight and EPS backing.

and Super High films, it was difficult to examine the magnitude and intensity of color on the film. These differences were caused by the inherent characteristic of the films. These films were designed for high pressure environments and the impacts observed by the sensor films in this research may not have caused pressure to exceed the threshold point of the films.

In terms of backing materials, extruded polystyrene foam panels showed clear and visible color difference as compared to the plastic corrugated sheet. In addition, the polystyrene sheet was better than plastic corrugated sheet to calculate the area and diameter of the pressure imprint on the films.

3.2 Phase II: Comparison of the Performance of Selected Combinations

Since not all the results from Phase I were very easy to interpret, this phase helped isolate the optimum combinations of sensor film and backing materials for further investigation. Ultra Low and Super Low sensor films with both the plastic corrugated sheets and EPS foam backing were further tested using the 3.6 kg (8 lb) spherical weight from four different drop heights of 0.45, 0.66, 0.86 and 1.22 m (18, 26, 34, and 48 in). The results are shown in Figures 7 and 8.



Ultra Low Film (Plastic Corrugated Sheet)

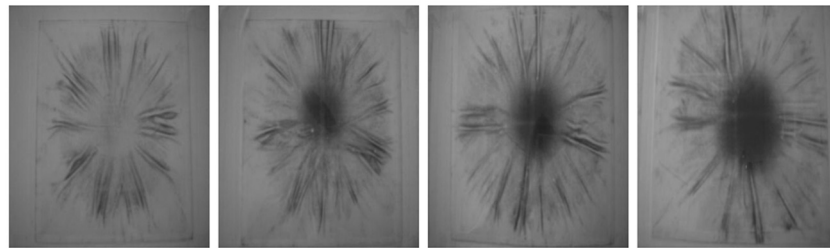
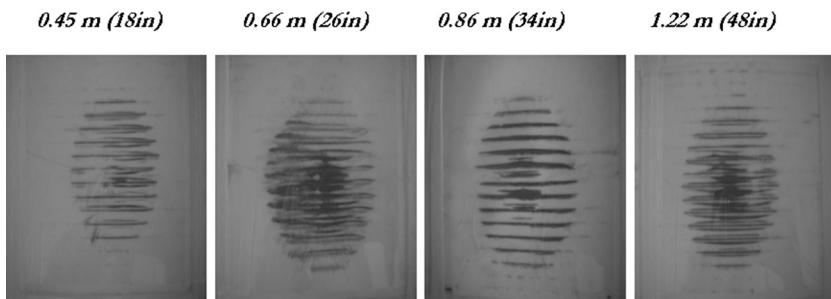
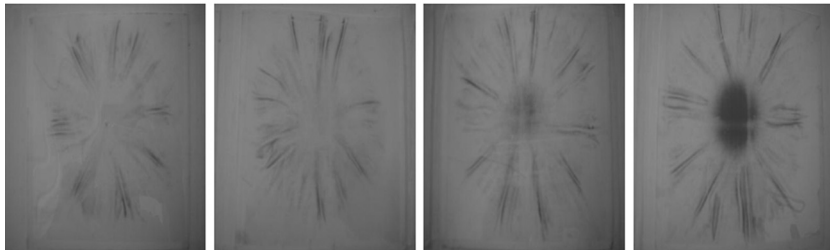


Figure 7. Results of Phase II testing for ultra low sensor film.



Super Low Film (Plastic Corrugated Sheet)



Super Low Film (EPS Backing)

Figure 8. Results of Phase II testing for super low sensor film.

3.3 Phase III: Quantification of Pressure Imprints and Derivation of Regression Relationships

Based on the results from the first and second phase testing, the Ultra Low film in conjunction with the two spherical weights and the Super Low film in conjunction with the 6.8 kg (15 lb) spherical weight were used to repeat the testing from three different drop heights, 0.61, 0.76 and 0.91 m (24, 30 and 36 in). The linear regression plots for the more prominent combinations of sensor film and backing materials are presented in Figure 9.

For the application of the sensor film to measure and predict dynamic shock values experienced during drops, a quantification of the pressure imprint on the film was used to develop linear regression relationships with the actual drop heights. In addition, the major objective of this research was to evaluate the feasibility of the sensor films as a cheaper substitute for higher cost dynamic drop testers. Based on the tests, these sensor films provide a simpler method of measuring and predicting package drops by evaluating the strength and pressure distribution profiles between two contacting surfaces.

Since the pressure imprints on the films are circular in shape (function of impact surface), the diameter and the subsequent area of the pressure mark were good candidates for the representation of the actual drop height. For this reason, the diameter and the area of the pressure imprints

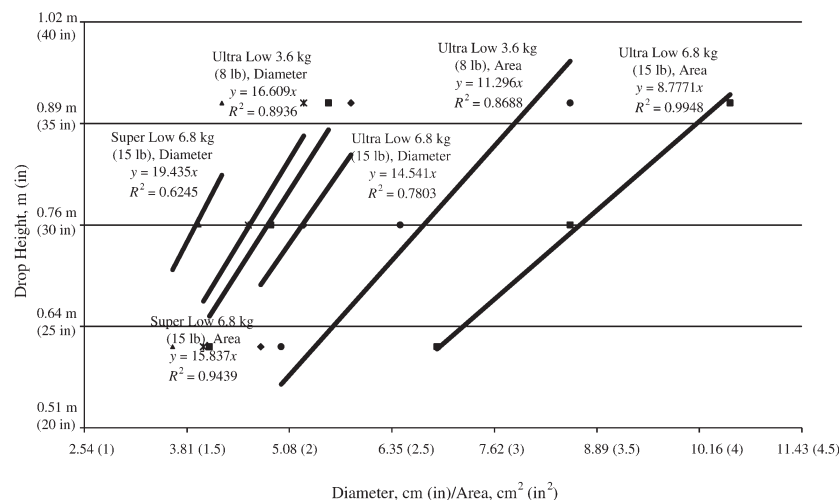


Figure 9. Linear regression relationships for Phase III testing.

on the film were tried as the indicators of the actual drop heights. Five replicates of the diameters of the pressure mark were measured for each film with specific drop height. Thereafter, the approximate area of the pressure marks was calculated.

The average diameters and areas were plotted with the actual drop height for each film. Each data set was analyzed with linear regression method. As shown in Figure 9, the R^2 values between the area and the drop height, which varies between 0.8688 and 0.9948, are much higher than those between the diameter and the drop height, which vary between 0.6245 and 0.8936. This means that area of imprint on the film was a better indicator of the actual drop height and could be used to predict actual drop heights.

For the R^2 values of the correlation between imprint area and the drop height, the result of the Ultra Low film showed better performance than Super Low film. The R^2 values for the Ultra Low film was 0.9948 and that for Super Low film was 0.9439 for the 6.8 kg (15 lb) weight. These results show that the measurement of the imprint area using Ultra Low film could be a better indicator of the drop heights.

This method can now be used with other shaped objects and actual products. Shippers can mount the pressure sensitive film on a foam backing and apply to the bottom surface inside a package. They can then calibrate the shaped object and imprint area as a function of drop height. Post damage analysis would require observing the film and measuring the size of imprinted area to predict safe or severe handling.

5.0 CONCLUSIONS

1. Ultra Low sensor film was the best to predict actual drops and associated heights and extruded polystyrene foam sheet was the best backing material based on this study.
2. While comparing the cushion materials, extruded polystyrene sheet was better in calculating the magnitude of area, color and clarity to evaluate the dispersion of pressure strength on the film.
3. The results showed that the pressure sensitive film is a useful method to predict drop height without any expensive instrumentation and can be successfully used as an indicator of the drop height in various distribution environments. These films can be used in shipments of expensive products to show evidence of severe impacts in case damage occurs.

REFERENCES

1. Sensor Product Inc. (2004) "Pressurex", Available at <http://www.sensorprod.com/pressurex.html>, accessed June 14, 2009.
2. ASTM D4169 - 08 (2008) Standard Practice for Performance Testing of Shipping Containers and Systems, Vol. 15.10, American Society of Testing and Materials, West Conshohocken, PA, USA, 2007.
3. ASTM D4332-01(2006), Standard Practice for Conditioning Containers, Packages, or Packaging Components for Testing, Vol. 15.10, American Society of Testing and Materials, West Conshohocken, PA, USA, 2007.

Method for Measuring the Oxygen Transmission Rate of Perforated Packaging Films

AYMAN ABDELLATIEF and BRUCE A . WELT*

*Packaging Science Program, Agricultural & Biological Engineering Department,
University of Florida, IFAS 111 Frazier Rogers Hall, Gainesville, FL 32611-0570*

ABSTRACT: A new method was developed to measure the Oxygen Transmission Rate (OTR) of perforations using fiber optic oxygen sensors. The method was used to measure the OTR of calibrated perforations with diameters of approximately 100, 150, 200, and 250 μm at 15, 23, and 30°C. The oxygen concentration was measured over time in a chamber which allowed oxygen to diffuse through the perforation over a concentration gradient. The plot of the logarithm of the ratio concentration gradient at time t to the initial concentration gradient yielded a straight line. The permeance was calculated from the slope of the line. The OTR is function of the oxygen concentration gradient and was calculated by multiplying the permeance by the concentration gradient at a particular time. The initial OTR is the largest value and goes to zero as the concentration in the chamber approaches ambient conditions. Permeance of perforations increased with increasing diameter but decreased with increasing temperature. This method could be used to measure OTR of perforated packaging films.

INTRODUCTION

FEW commercially available films have sufficiently high oxygen transmission rates for packaging of respiring products. Many fruits and vegetables, such as strawberries and mangos have high respiration rates which makes it difficult to supply sufficient oxygen through packaging films without perforations. Films with perforations on the order of 40 to 250 μm are generally referred to as micro-perforated films. Design of packages using micro-perforated films has been difficult due to lack of methods capable of properly measuring OTR of films with perforations.

* Author to whom correspondence should be addressed. Email: bwelt@ufl.edu

Difficulties measuring OTR of perforated films with traditional approaches is evident. Figure 1 shows the coulometric approach that is the basis of current commercial instrumentation. The figure shows a test where oxygen would permeate from right to left through the sample film mounted in the middle.

Test films split the test chamber into two halves. An oxygen containing gas (test gas) flows on one side while an oxygen free gas (carrier gas) flows on the other. This system works well for film samples without perforations since slight variations of pressure on either side of the sample do not significantly alter measurements. However, when perforations exist, variations in pressure cause gas to flow freely from one side to the other, which directly affects measurements. It is difficult to design this approach to work reliably for perforated films because it would require exactly equal flow rates for the carrier gas and test gas which would require very precise control of flow rates.

Figure 2 shows an alternative method for measuring OTR, which requires headspace sampling over time. Actual experiments often require removal of multiple samples from a single test specimen. Without perfor-

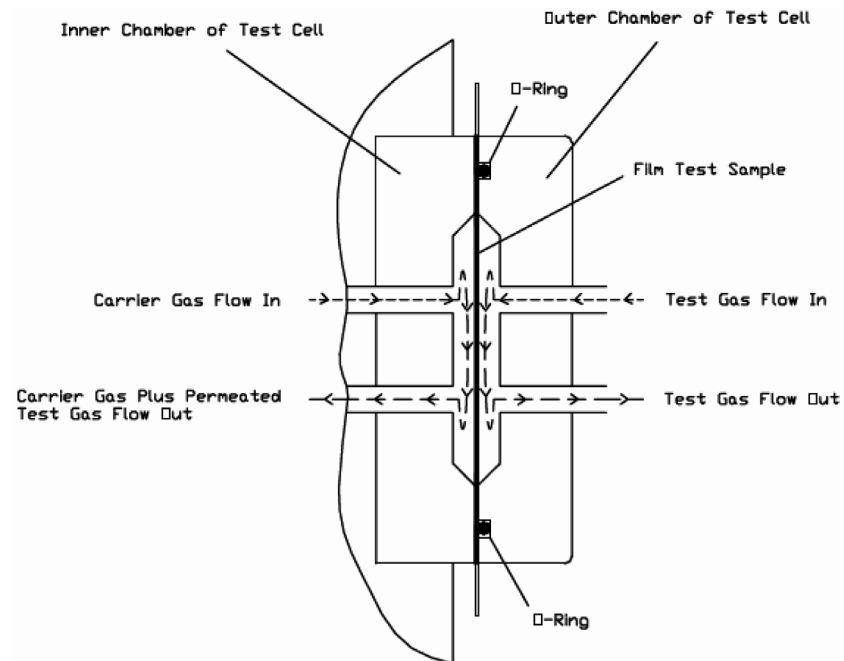


Figure 1. Typical apparatus for measuring OTR using coulometric method.

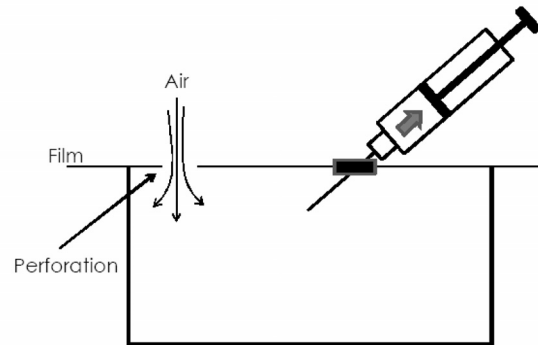


Figure 2. Unsteady state measurement of headspace over time.

rations, each sampling changes headspace volume, which affects the measurement. With perforations, each sample draws new gas into the headspace, changing gas compositions, thus affecting subsequent samples. To overcome these difficulties, a new approach was developed using a fluorescence based fiber optic sensor that is capable of continuously measuring gas within the test apparatus without removing or consuming gas and without a need for continuously flowing gases.

THEORY

Attempts to predict transmission rates of gases through perforated films have been made. Emond and others, (1991) and Fonseca and others, (1996) used empirical models to describe diffusion of gases through perforated films. Fishman and others, (1996) modeled transmission rates of gases using Fick's law of diffusion, while Hirata and others, (1996) used Graham's law of diffusion. Renault and others, (1994a) modeled diffusion of gas through perforated films with Maxwell Stefans law. Ghosh and Anantheswaran (1998) determined that models based on Fick's law were in closest agreement with experimental data.

Oxygen Transmission Rate (OTR) Measurements

Non-perforated Films

Ghosh and Anantheswaran (1998) reviewed four methods used to determine OTR. These methods include (1) manometric (ASTM D1434, 1995), (2) volume (ASTM D1434, 1995), (3) coulometric sensor

method (ASTM D3985, 1995) and (4) concentration increase methods (Landrock and Procter 1952; Moyls and others, 1992).

Both manometric and volume methods rely on the same type of apparatus. Neither approach is appropriate for perforated films, so these are only briefly described here. A sample is mounted in a gas transmission cell to form a sealed semibarrier between two chambers. One chamber contains test gas at a specific high pressure, and the other chamber at a lower pressure receives the permeating gas. In the Manometric method the lower pressure chamber is evacuated and transmission of the gas through the film is indicated by an increase in pressure. In the volume method the lower pressure chamber is maintained at atmospheric pressure and the gas transmission is indicated by a change in volume.

The coulometric method Figure 1 involves mounting a specimen as a sealed semibarrier between two chambers at atmospheric pressure. One chamber is purged with a non oxygen containing carrier gas such as nitrogen, and the other chamber is purged with oxygen containing test gas, which is typically air (21% oxygen) or 100% oxygen. Oxygen permeates through the film into the carrier gas, which is then transported to a coulometric sensor. Oxygen is consumed in a process that generates an electric current proportional to the amount of oxygen flowing to the sensor in a given time period.

The concentration increase method is an unsteady state method whereby the chamber is sealed with a semi-barrier and is initially purged with an oxygen free gas such as nitrogen. Oxygen diffuses through the barrier and the concentration of oxygen is measured over time. The most common method used to measure the oxygen concentration is a gas chromatograph, which requires removal of gas samples from the test chamber (Figure 2) using a syringe.

Perforated Films

The volume and manometric methods involve a pressure differential which would cause gas to flow through perforations, rendering these methods unsuitable for OTR measurements of perforated films. The coulometric method has basic physical limitations (Johnson and Demorest 1997) and becomes impractical for very high OTRs even without perforations due to costly sensor consumption. Perforations create additional challenges due to practical difficulties of avoiding non-diffusional gas flow through perforations. The approach developed in this work is an enhancement of the typical concentration increase

method. This approach is superior to other methods since the measurement does not rapidly consume the sensor, the sensor does not consume gases involved in the measurement, the apparatus does not require consumption of constantly flowing gases, and the approach does not create or rely upon pressure differentials.

Fiber Optic Oxygen Sensor

Sensors based on oxygen quenching fluorophores are commercially available. Typically fluorophores are suspended in sol gel complex and mounted at the tip of a fiber optic probe. Oxygen probes available from Ocean Optics Inc. (Dunedin, FL) use a fluorescing ruthenium complex. For durability, probes may be mounted in steel shafts of varying diameter in a manner that resembles hypodermic needles. For this work 18 gauge probes were used (Model FOXY 18G, Ocean Optics Inc, Dunedin, FL). A pulsed blue LED sends light, at 475 nm, onto an optical fiber. The optical fiber carries the light to the probe tip, which excites the fluorophore causing an emission at ~600 nm. Excitation energy is also transferred to oxygen molecules in non-radiative transfers. Therefore oxygen decreases or quenches the fluorescence signal (Kautsky 1939). Fluorescent energy is collected by the probe and carried through the optical fiber to spectrometer.

Degree of fluorescence quenching relates to the frequency of collisions, and therefore concentration, pressure and temperature of the oxygen-containing media. A fluorescence quenching based sensor was selected for use in this method primarily because it can measure oxygen concentration without consuming oxygen. Other methods require removal of gas from the system or consumption of oxygen, which directly affects the measurement.

MATERIALS AND METHODS

The apparatus for measuring OTR was divided into in three parts, which, in this case, were fabricated mainly from magnesium metal, which was readily available in our machine shop, but can be fabricated from any metal (Figure 3). The bottom incorporates a transparent plastic window in order to allow for a magnetic stir bar in the test chamber. The height of the middle section is 5 cm and is a hollow cylinder with four ports for flushing with nitrogen and compressed air, mounting the fiber

optic oxygen probe, and to provide for a gas outlet valve. The middle also accommodated o-rings for gas tight seals with top and bottom. The top is a ring with a precise open area of 50 cm² to accommodate film samples. Figure 3 shows a diagram of the OTR measurement chamber.

Measurement of Samples

Stainless steel disks 0.02 inches thick with precision orifices were procured (FSS-318-cal-100, 150, 200, 250, Lenox Laser, Glen Arm, MD) and used to test the apparatus since we found it difficult to repeatedly produce consistent holes with desired geometry in our laboratory. Hole diameters were 100, 153, 205, and 249 μm . Oxygen partial pressure in the chamber was recorded every 10 seconds using the average of four measurements with the fiber optic oxygen sensing system. Measurements were made at 15°C, 23°C, and 30°C inside a computer controlled environmental chamber. Transmission of oxygen through the film and orifice can be modeled as follows

$$\frac{dn_{\text{O}_2}}{dt} = \frac{\bar{P}_{\text{O}_2} A}{l} (p_{\text{O}_2}^{\text{air}} - p_{\text{O}_2}^t) \quad (1)$$

For the case of perforated films, diffusion of oxygen and nitrogen experience similar partial pressure gradients ranging from 0.21 to 0 (Figure 4).

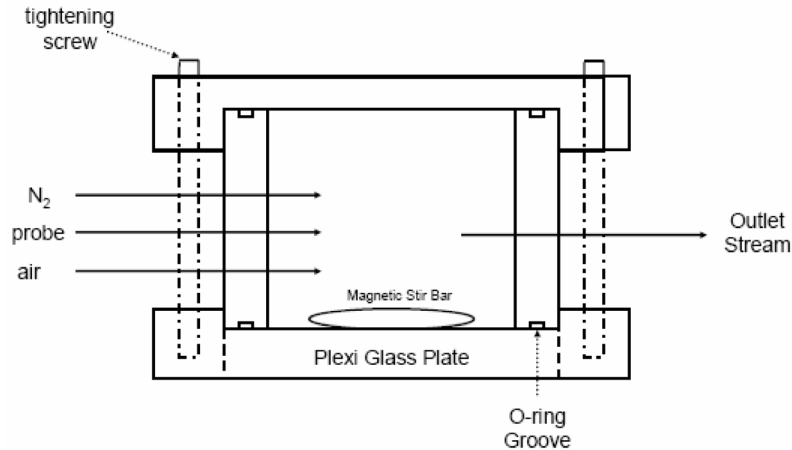


Figure 3. Schematic profile of OTR chamber.

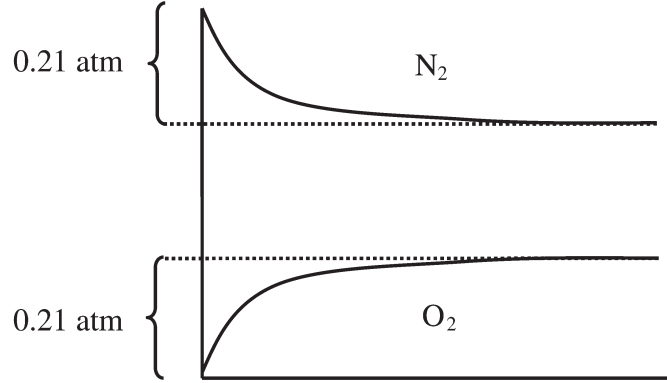


Figure 4. Driving force for oxygen and nitrogen concentration.

Therefore, for perforated films, gas transfer rates of oxygen and nitrogen are similar.

$$\frac{dn_{O_2}}{dt} \cong \frac{dn_{N_2}}{dt} \quad (2)$$

For a rigid test apparatus with a perforated film mounted, volume and pressure are constant. Therefore, oxygen partial pressure can be related to moles of oxygen via the ideal gas law

$$p_{O_2} = \frac{n_{O_2} RT}{V_{tot}} \quad (3)$$

Substituting Equation (3) into Equation (1)

$$\frac{dp_{O_2}}{dt} = \frac{RT}{V_{tot}} \cdot \frac{\bar{P}_{O_2} A}{l} (p_{O_2}^{air} - p_{O_2}^t) \quad (4)$$

Integrating Equation (4) provides

$$\ln \left[\frac{p_{O_2}^{air} - p_{O_2}^t}{p_{O_2}^{air} - p_{O_2}^0} \right] = \frac{RT}{V_{tot}} \cdot \frac{\bar{P}_{O_2} A}{l} t \quad (5)$$

Taking the value of the slope of a plot of $\ln[(p_{O_2}^{air} - p_{O_2}^t)/(p_{O_2}^{air} - p_{O_2}^0)]$ versus t and solving for permeance, \bar{P}_{O_2} / l , yields

$$\frac{\bar{P}_{O_2}}{l} = \frac{|slope|V_{tot}}{RTA} \quad (6)$$

Permeance can be converted to volumetric units by multiplying by the molar volume of gas derived from the ideal gas law. Oxygen transmission rate, OTR , is the product of permeance and partial pressure difference, Δp .

$$OTR = \frac{\bar{P}_{O_2}}{l} (p_{O_2}^{air} - p_{O_2}^t) \quad (7)$$

Since Δp changes throughout the unsteady state experiment, the result is a plot that provides OTR as an asymptotic function of Δp . During an experiment, OTR is greatest when Δp is greatest (Figure 6), which is at the beginning of the experiment when the apparatus is flushed with nitrogen. OTR tends to zero as gas in the vessel approaches the composition of the ambient gas. This plot can then be used to design perforated packages when a particular internal oxygen concentration (Δp) is desired.

RESULTS AND DISCUSSION

For the case of a calibrated 249 μm orifice at 30°C, a plot of $\ln[(p_{O_2}^{air} - p_{O_2}^t)/(p_{O_2}^{air} - p_{O_2}^0)]$ versus t yielded a curve approximated by a straight line.

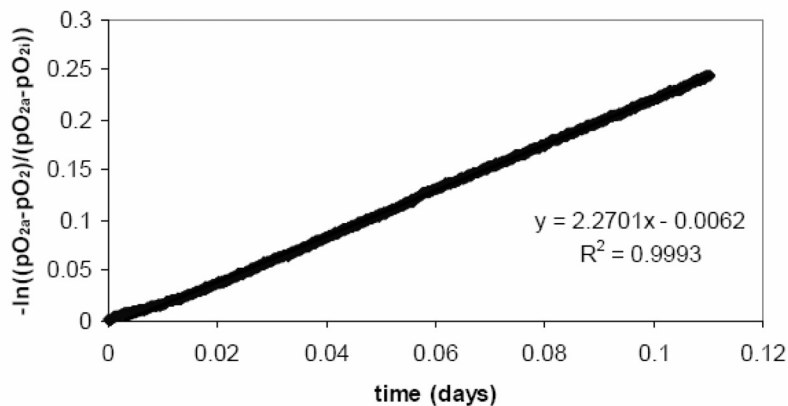


Figure 5. Plot used to determine permeance of hole/perforation 249 μm hole at 30°C.

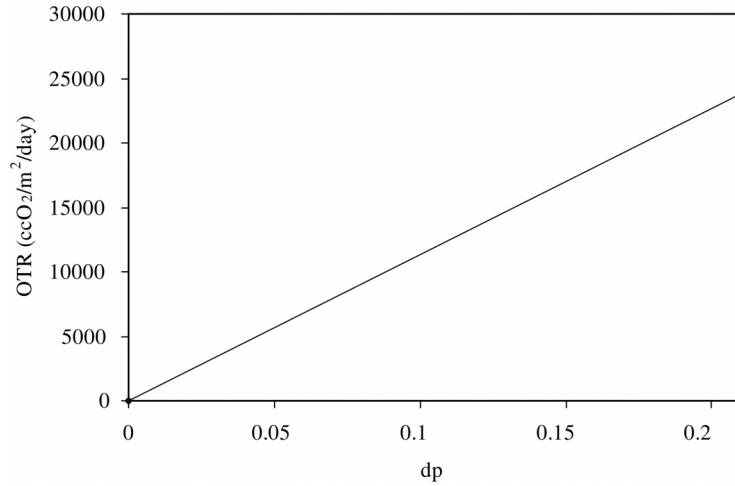


Figure 6. OTR vs Δp.

Calculating the permeance from Equation (6) and converting to volumetric units yields

$$\frac{\bar{P}_{O_2}}{l} = 1.135 \times \frac{10^5 \text{ cc O}_2}{\text{m}^2\text{-atm-day}}$$

Figure 6 shows that *OTR* is greatest at the beginning of the experiment when the oxygen partial pressure in the chamber is zero and the *OTR* goes to zero as the concentration inside the chamber reaches ambient concentration.

Figure 7 shows the permeance, for duplicate measurements, for all

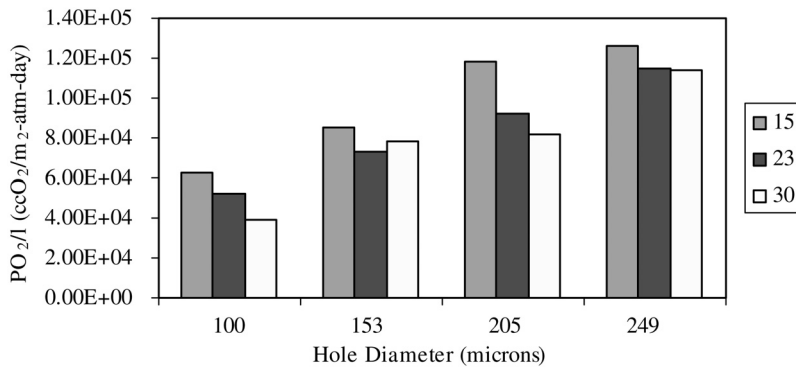


Figure 7. \bar{P}_{O_2}/l vs. temperature (°C).

holes at three different temperatures (15°C, 23°C, 30°C). The figure primarily shows that the apparatus is capable of providing consistent and reliable measurements. Additionally, the figure shows a tendency for *OTR* to decrease with increasing temperature, despite the fact that gas diffusion coefficients are generally known to increase with temperature. It is likely that reduced gas density at higher temperatures offset increases in gas diffusion coefficients

CONCLUSION

Measurements of *OTR* through precision holes proved to be consistent and reproducible. This provides confidence that this approach can be extended to accurately measure *OTR* in microperforated packaging films where such microperforations tend to be dimensionally irregular. This device can be used to design packaging for respiring produce which require a specific oxygen partial pressure in the package.

NOMENCLATURE

- t = time (days)
- n_{O_2} = moles of O_2
- n_{N_2} = moles of N_2
- \bar{P}_{O_2} / l = permeability of O_2 ((mole O_2 -mil)/(atm-m²-day))
- l = thickness of film (mil)
- $P_{O_2}^{air}$ = oxygen partial pressure in air (atm)
- $P_{O_2}^t$ = oxygen partial pressure at a given time (atm)
- $P_{O_2}^0$ = initial oxygen partial pressure (atm)
- V_{tot} = total volume of vessel (cc)
- A = area (m²)
- R = gas law constant 82.06 cc-atm/mol-day
- T = absolute temperature (Kelvin)
- OTR = mole O_2 /m² day

REFERENCES

1. Emond, J.P. 1992. Mathematical modeling of gas concentration profiles in perforation-generated modified atmosphere bulk packaging. Ph.D. Thesis, University of Florida.
2. Emond, J.P., Castaigne, F., Toupin, C.J. and Desilets, D. 1991. Mathematical modeling of gas exchange in modified atmosphere packaging. *Trans. ASAE*. 34(1), 239–245.

3. Fishman, S., Rodov, V. and Ben-Yehoshua, S. 1996. Mathematical model for perforation effect on oxygen and water vapor dynamics in modified atmosphere packages. *Journal of Food Science* 61(5), 956–961.
4. Fonseca, S.C., Oliviera, F.A.R. and Chau, K.V. 1996. Oxygen and carbon dioxide exchange through a perforation, for development of perforated modified atmosphere bulk packages. Poster presented at Ann. Mtg., June 22–26, Institute of Food Technologists, New Orleans, LA.
5. Ghosh, V. and Anantheswaran, R.C. 2001. Oxygen Transmission Rate through Micro-Perforated Films: Measurement and Model Comparison. *J. Food Process Engineering*. 24.
6. Hirata, T., Makino, Y., Ishikawa, Y., Katusara, S. and Hasegawa. 1996. A theoretical model for designing a modified atmosphere packaging with a perforation. *Trans. ASAE*. 39(4), 1499–1504.
7. Kautsky, H. (1939) Quenching of luminescence by oxygen. *Trans. Faraday Soc.*, 35, 216–219.
8. Landrock, A.H. and Procter, B.E. 1952. The simultaneous measurement of oxygen and carbon dioxide permeabilities of packaging materials. *Tappi*. 35(6), 241–246.
9. Lee D.S., P.E. Hagger, J. Lee, and K.L. Yam 1991. 'Model for Fresh Produce Respiration in Modified Atmosphere Based on Principle of Enzyme Kinetics', *Journal of Food Science* Vol. 56 No. 6, 1580–1585.
10. Moyls, L., Hocking, R., Beveridge, T. and Timbers, G. 1992. Exponential decay method for determining gas transmission rate of films. *Trans. ASAE*. 35(4), 1259–1265.
11. Renault, P., Souty, M. and Chambroy, Y. 1994a. Gas exchange in modified atmosphere packaging. 1: A new theoretical approach for microperforated packs. *Intern. J. Food Sci. Technol.* 29, 365–378.

GUIDE TO AUTHORS

1. Manuscripts shall be sent electronically to the editor, Dr. Jay Singh at singhjapr@gmail.com using Microsoft Word in an IBM/PC format. If electronic submission is not possible, three paper copies of double-spaced manuscripts may be sent to Jay Singh, Industrial Technology, Cal Poly State University, San Luis Obispo, CA 93407. (Telephone 805-756-2129). Manuscripts should normally be limited to the space equivalent of 6,000 words. The editor may waive this requirement on special occasions. As a guideline, each page of a double-spaced manuscript contains about 300 words. Include on a separate title page the names, affiliations, and addresses of all the authors, and identify one author as the corresponding author. Because communication between the editor and the authors will be electronic, the email address of the corresponding author is required. Papers under review, accepted for publication, or published elsewhere in journals are normally not accepted for publication in the *Journal of Applied Packaging Research*. Papers published as proceedings of conferences are welcomed.
2. Article titles should be brief, followed by the author's name(s), affiliation, address, country, and postal code (zip) of author(s). Indicate to whom correspondence and proofs should be sent, including telephone and fax numbers and e-mail address.
3. Include a 250-word abstract and 5–6 keywords.
4. If electronic art files are not supplied, submit three copies of camera-ready drawings and glossy photographs. Drawings should be uniformly sized, if possible, and planned for 50% reduction. Art that is sent electronically should be saved in either a .tif or .JPEG format for superior reproduction. All illustrations of any kind must be numbered and mentioned in the text. Captions for illustrations should all be typed on a separate sheet(s) and should be understandable without reference to the text.
5. DEStech uses a numbered reference system consisting of two elements: a numbered list of all references and (in the text itself) numbers in brackets that correspond to the list. At the end of your article, please supply a numbered list of all references (books, journals, web sites etc.). References on the list should be in the form given below. In the text write the number in brackets corresponding to the reference on the list. Place the number in brackets inside the final period of the sentence cited by the reference. Here is an example [2].

Journal: 1. Halpin, J. C., "article title", *J. Cellular Plastics*, Vol. 3, No. 2, 1997, pp. 432–435.

Book: 2. Kececioglu, D. B. and F.-B. Sun. 2002. *Burn-In Testing: Its Quantification and Optimization*, Lancaster, PA: DEStech Publications, Inc.

6. Tables. Number consecutively and insert closest to where first mentioned in text or type on a numbered, separate page. Please use Arabic numerals and supply a heading. Column headings should be self explanatory and carry units. (See example at right.)
7. Units & Abbreviations. SI units should be used. English units or other equivalents should appear in parentheses if necessary.
8. Symbols. A list of symbols used and their meanings should be included.
9. Page proofs. Authors will receive page proofs by E-mail. Proof pages will be in a .PDF file, which can be read by Acrobat Reader. Corrections on proof pages should be limited to the correction of errors. Authors should print out pages that require corrections and mark the corrections on the printed pages. Pages with corrections should be returned by FAX (717-509-6100) or mail to the publisher (DEStech Publications, Inc., 439 North Duke Street, Lancaster, PA 17602, USA). If authors cannot handle proofs in a .PDF file format, please notify the editor, Jay Singh at singhjapr@gmail.com.
10. Index terms. With proof pages authors will receive a form for listing key words that will appear in the index. Please fill out this form with index terms and return it to the publisher.
11. Copyright Information. All original journal articles are copyrighted in the name of DEStech Publications, Inc. All original articles accepted for publication must be accompanied by a signed copyright transfer agreement available from the journal editor. Previously copyrighted material used in an article can be published with the written permission of the copyright holder (see #14 below).
12. Headings. Your article should be structured with unnumbered headings. Normally two headings are used as follows:

Main Subhead: DESIGN OF A MICROWAVE INSTALLATION

Secondary Subhead: Principle of the Design Method

If further subordination is required, please limit to no more than one (*Third Subhead*).

13. Equations. Number equations with Arabic numbers enclosed in parentheses at the right-hand margin. Type superscripts and subscripts clearly above or below the baseline, or mark them with a caret. Be sure that all symbols, letters, and numbers are distinguishable (e.g., "oh" or zero, one or lowercase "el," "vee" or Greek nu).
14. Permissions. The author of a paper is responsible for obtaining releases for the use of copyrighted figures, tables, or excerpts longer than 200 words used in his/her paper. Copyright releases are permissions to reprint previously copyrighted material. Releases must be obtained from the copyright holder, which is usually a publisher. Forms for copyright release will be sent by the editor to authors on request.

General: *The Journal of Applied Packaging Research* and DEStech Publications, Inc. are not responsible for the views expressed by individual contributors in articles published in the journal.

Table 5. Comparison of state-of-the-art matrix resins with VPS/BMI copolymers.

Resin System	Core Temp. (DSC peak)	Char Yield, %
Epoxy (MY720)	235	30
C379: H795 = 1.4	285	53